Device model for pulsing in silicon *p-i-n* structures

A. G. U. Perera and S. Matsik
Department of Physics and Astronomy, Georgia State University, Atlanta, Georgia 30303

(Received 7 July 1993; accepted for publication 9 December 1993)

We report experimental data and modeling results based on device physics and circuit parameters for the spontaneous firing patterns for silicon *p-i-n* structures at 4.2 K controlled by a constant current source. The model provides insights into the sensitivity of the pulsing rate and explains the wide range of behavior observed. The knowledge on the effect of these parameters on pulsing is critical for designing uniform arrays, which will have a major impact on applications such as infrared detectors and neural net models. The model will also serve as the first step towards obtaining high temperature pulsing arrays using quantum well structures.

Here, we report a theoretical model to explain effects associated with nonlinear dynamics in circuits containing silicon *p-i-n* diodes at 4.2 K under constant driving current. The circuits generate spiketrains and are qualitatively similar to neuron equivalent circuits.[1] These pulsing structures have been used as novel infrared (IR) detectors[2] without any preamplifiers, as artificial neurons,[1] and in neural net based parallel asynchronous processors.[3] All of these applications were tested on commercial diodes which showed large variations in the pulsing phenomena, from no pulsing at all, to large variations in pulse rate and patterns. This leads us to believe that some parameters are extremely important for this pulsing phenomena. An understanding of these variations is important if devices with uniform behavior are to be fabricated for use in applications such as IR detector arrays or neural networks. The extension of this behavior to higher temperature, through the use of quantum well structures or δ-doped *p-i-n* structures which have already been used for IR detection,[4] could lead to a wide range of practical applications.

The nonlinear dynamics mechanism involves a low injected current causing a slow buildup of space charge by impact ionization while the input capacitor is charged. This is followed by a fast transition to high injected current, neutralizing the accumulated space charge and discharging the input capacitor. The dependence on the diode and circuit parameters has been analyzed for purely periodic pulsing.[5] These nearly uniform fast ~1 V pulses (risetime ~90 ns) occur at variable intervals due to varying neutralization of the space charge. These interpulse time intervals (IPTIs) define a time series. We use a latching scalar to count the pulses from a fast clock ($\leqslant$10 MHz) between the diode pulses which gives a resolution of up to 0.1 μs. Models have been proposed for current oscillations in bulk semiconductor material.[6] However, only a few models have tried to understand pulsing.[5] Here we consider a model to determine the crucial device parameters for IPTIs. Experimental IPTIs were used (by fitting to the model) to obtain two critical parameters for pulsing, the initial space-charge layer thickness and the thickness of the *n-i* interface. Predictions are also made for the purpose of device fabrication.

The model determines the time at which a pulse occurs for a set of initial conditions, most of which are fixed by the device parameters and circuit elements; only the initial space charge can vary from pulse to pulse at a given current. Since the initial space charge for a pulse is taken as a free parameter in the model, we do not predict the variation in successive IPTIs, but rather the average value for a given current. The interface thickness d[7] (a measure of the sharpness of the interface[1]) will vary with the current. However, it should be constant at a given current. When more than one average value is available, as in the case of bimodal pulsing, a fit is made for each of the values. Since the approach is based on our previous work[5] only the major equations are given here. However, as we expand the model more details will be given.

The model assumes that a slow buildup of space charge characterized by a low electron injection current, is followed by a fast high electron injection current pulse during which some of the space charge is neutralized, resetting the diode for the next pulse. This space-charge layer of thickness w and the resulting band diagram are shown in Fig. 1. The voltage across the diode is given by

$$V_{\text{diode}}=\frac{A}{C}\int_{t_i}^{t_f}(i_T-j\,)dt-\frac{A}{C_L}\int_{t_i}^{t_f}j dt,$$

with i_T the input current density (A/m^2), j the injection current density, and C_L and C the load and input capacitances, neglecting the discharge of the load capacitor through the

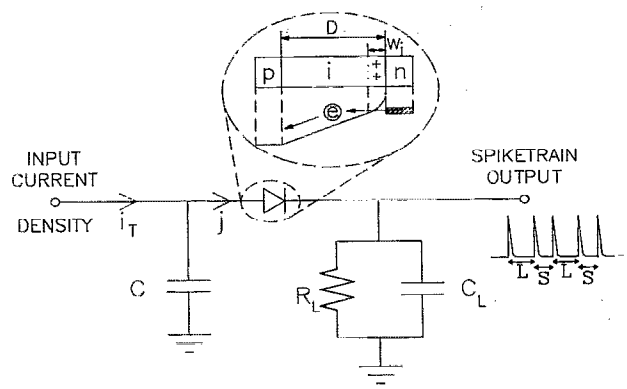

FIG. 1. The simple circuit used to obtain the spontaneous pulsing. The diode is driven by a dc current at 4.2 K. $C_L\simeq$100 pF and $C\simeq$100 pF are due to the cables and $R_L\simeq$300 kΩ. The inset shows the space-charge distribution and the resulting band diagram for the diode.

 0003-6951/94/64(7)/878/3/$6.00

load resistor. This is valid as $R_L C_L (\sim 50\ \mu s) \ll$ IPTIs (1–100 ms). Another expression for the voltage across the diode is $V_{\text{diode}} - V_0 = ED + V_{\text{bi}}$, where E is the field across the i region, $V_{\text{bi}} = \text{new}_i^2/(2\epsilon)$ is the built-in potential[8] due to the i-region space charge and $V_0 = 1.1$ V is the flatband voltage for Si.

The space-charge buildup is given by $dw/dt = [(D-w)/e]\sigma j$, and σ is the impact ionization cross section.[9] Combining the above equations we obtain

$$\frac{Ai_T t}{C} - \frac{Ae(w-w_i)(C+C_L)}{(D-w_i)\sigma C C_L} = ED + V_0 + \frac{w^2 en}{2\epsilon}. \quad (1)$$

The injection current density is given by a modified[7] Richardson–Dushman equation $j = A^* T^2 \exp(\Delta - edF/kT)$, where Δ is the interfacial work function at the n-i interface[7] and F is the field at the n-i interface. Assuming uniform distribution of impurities ($\rho = ne$), we can calculate the field at the n-i interface. This choice for the space charge is where the present work deviates from the previous results. It is based on numerical results which indicate the space charge forms a fully ionized region at the n-i interface with minimal ionization in the rest of the i region. Combining these results and linearizing the equations with the approximation $\Delta w = |w - w_i| \ll w_i$, we find the temporal dependence of w to be

$$\exp[(\beta-\gamma)w] = \theta + R[(\beta-\gamma)/\alpha]\exp(\alpha t)$$

in terms of the constants:

$$\alpha = Aedi_T/CDkT,$$

$$\beta = Ae^2 d/CDkT(D-w_i)\sigma,$$

$$\gamma = ne^2 d(D-w_i)/D\epsilon kT,$$

$$\theta = \exp[(\beta-\gamma)w_i] - R(\beta-\gamma)/\alpha,$$

$$R = \exp(\beta w_i)\exp\left[\frac{ne^2 dw_i^2}{2D\epsilon kT}\right]\eta,$$

where

$$\eta = [(D-w_i)e]\sigma A^* T^2 \exp[-(\Delta + edV_0/D)/kT].$$

The approximations used in reaching this result will hold for most of the time between pulses. During the pulse itself, the approximations may break down. However, because the measured variation in the IPTIs is generally much larger than the length of the pulse, we can ignore the portion of the pulse in which the approximation fails.

Depletion will continue efficiently as long as the electric field efficiently sweeps carriers out of the n region, i.e., until $E = 0$. Substituting the above expression in Eq. (1) and setting $E = 0$, we obtain an expression which describes the relationship between the firing time interval and input current density with the device parameters:

$$\frac{Ai_T t}{C} - (G+M)\ln\left(\theta + \frac{R(\beta-\gamma)}{\alpha}\exp(\alpha t)\right) + G_1 = 0, \quad (2)$$

where

$$G = Ae(C+C_L)/CC_L(D-w_i)\sigma(\beta-\gamma),$$

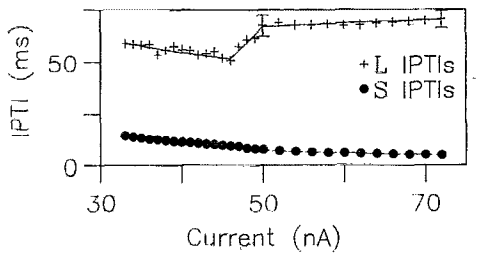

FIG. 2. Plot of both L and S IPTI vs driving current. The points were determined from averaging the IPTI data. The theoretical fit was obtained by a least-squares fit in the low and high current regions. The dashed lines indicate the regions used to obtain the fits. The center region values were determined by connecting the endpoints of the d and w_i values determined for the other two regions. The error bars for the L IPTIs vary from 8 to 4 ms. They were not drawn for S, since the values vary only from .8 to .4 ms.

$$M = enw_i/2\epsilon(\beta-\gamma),$$

and

$$G_1 = G(\beta-\gamma)w_i - V_0 + enw_i^2/2\epsilon.$$

This can be solved numerically for the IPTIs.

This model is used to explain the experimental results from a sample consisting of a $D = 150$-μm-thick, 10^{14} cm^{-3}-doped Si:P i region, sandwiched between 1-μm-thick Si:P and Si:B regions, with an $A = 1$ mm^2 cross-sectional area. The known circuit parameters used were C and $C_L = 150$ pF, $R_L = 300$ kΩ. The data consisted of sets of 2100 IPTIs taken for drive currents between 33 and 72 nA at 1 or 2 nA intervals. A forbidden region in the IPTI distribution allows us to define the IPTIs as short (S) or long (L) whose mean values are shown in Fig. 2.

The initial values of w_i and d were varied to fit the mean values of the experimental data. The data were split into three regions based on the pattern of the IPTIs, below 46 nA, between 46 and 50 nA and above 50 nA. No fitting was done between 46 and 50 nA since there were only 3 data points available. These values were modeled by $w_i = w_{i0} + (\Delta w_i/\Delta i_T)i_T$ and $d = d_0 + (\Delta d/\Delta i_T)i_T$ with the zero current values w_{i0} and d_0, and the slopes $\Delta w_i/\Delta i_T$ and $\Delta d/\Delta i_T$ determined by a least-squares fit to the data in each segment. A fit for the S IPTIs was determined first since they were much less noisy than the L IPTIs. When this was done, we found $d(\text{nm}) = 70 - 10 i_T$ agrees with the data in both regions. This gives $69.3 \leqslant d \leqslant 69.7$ nm over the current region considered. The decrease in d with increasing current can be understood as an effect of the increasing field at the n-i interface needed to maintain the higher mean current. The initial depletion width was $w_{iS}\ (\mu\text{m}) = 1.721 + 2.15 i_T$ in the 33–46 nA range and $w_{iS}\ (\mu\text{m}) = 1.786 + 1.18 i_t$ in the 50–72 nA range. We expect d to be constant for a given current so the same value is used for the L IPTIs as for the S IPTIs. However, w_i can be different for 2 cycles at a given current, with the fit for the L IPTIs giving, $w_{iL}(\mu\text{m}) = 1.62 - 8.2 i_T$ in the 33–46 nA range and $w_{iL}\ (\mu\text{m}) = 2.06 - 22 i_T$ in the 50–72 nA range. The IPTI fit is shown by the lines in Fig. 2. The values between 46 and 50 nA were found by connecting the ends of

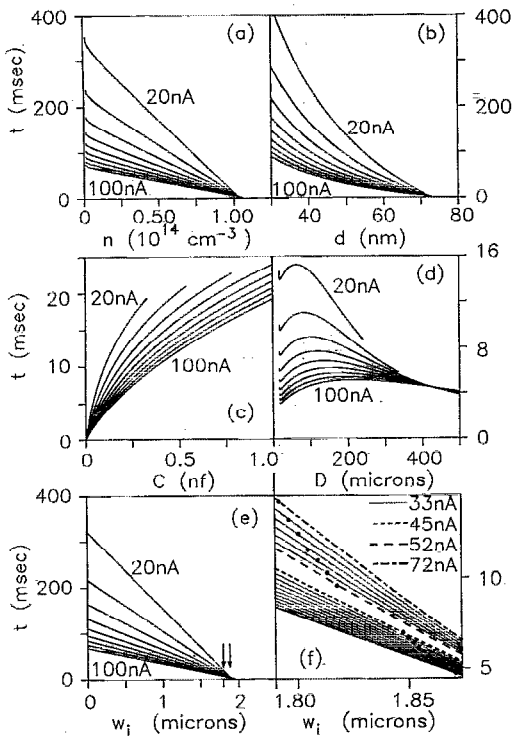

FIG. 3. The variation of the IPTIs with the various diode parameters and circuit elements for current between 20 and 100 nA. The parameters varied were (a) n, (b) d, (c) C, (d) D, and (e) w_i. (f) Expansion of the region marked by arrows in (e) with the experimental IPTIs marked as points along 2 nA current interval model outputs. The values for the constant parameters are $D=150$ μm, $d=70-10i$ nm, $w_i=1.83$ μm, $n=1\times10^{14}$ cm^{-3}, $A=1$ mm^2, $C=150$ pf, and $C_L=150$ pf. The cutoffs at high parameters values and at low paramcter values for D and n represent regions which have no pulsing solutions.

the fits to w_i and d. The variation of w_i with current could be an effect of the space-charge recombination phase of the pulse.

We have varied the parameters in Eq. (2) to see the effect on the IPTIs. All the parameters in the diode and the circuit except for R_L, which does not enter into the final equation, were varied. The results of these variations for currents between 20 and 100 nA are shown in Fig. 3. The variations with A and C_L are not shown since they are small. All the curves shown had a cutoff value above which pulsing would not occur. In addition, D and n also had a minimum value below which pulsing was not obtainable, probably caused by the inability of the i region to contain sufficient space charge. The large value cutoffs are probably related to the existence of a steady state with high injection current. These limits on pulsing varied with drive current. The existence of such limits for diodes to exhibit pulsing behavior has been observed experimentally. The IPTIs varied most for variations of w_i, d, and n, and least for variations of C_L and A. Of significance for fabrication is d which depends on the fabrication method.

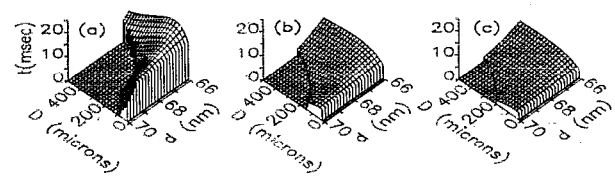

FIG. 4. The IPTI variation with D and d for (a) 20, (b) 60, and (c) 100 nA driving current. The sharp drop indicates the cutoff for the existence of pulsing solutions.

Figure 4 shows the variation of the IPTIs with D and d. The sharp drop in this plot shows the cutoff in the pulsing. Both the variations in the cutoff and the changes in the variation of the IPTIs with current are visible.

In conclusion, we have developed a model for pulsing in p-i-n diodes based on the circuit and device physics to explain the phenomena observed. This model provides an explanation for the sensitivity of the pulsing phenomena to various device and circuit parameters. It also places limits on most of the parameters in order for pulsing to occur. In particular, the fact that for the experimental data both n and d are close to the limit for pulsing to occur may provide an explanation for the fact that not all diodes with the same nominal parameters pulse. A small variation in either of these parameters could lead to the disappearance of pulsing behavior. Careful control of these parameters by use of fabrication techniques such as molecular beam epitaxy growth[10] will be needed to obtain uniform arrays. The extension of this work to higher temperatures by the use of MBE grown multiquantum well structures should be possible, since s-type negative differential conductivity has been observed[11] which was related to pulsing.[6] Such structures could use the impact ionization of impurities in the wells to produce the space-charge effects needed for pulsing at temperatures higher than those possible with p-i-n diodes.

This work was supported in part by the U. S. National Science Foundation under Grant No. ECS-9296238.

[1] D. D. Coon and A. G. U. Perera, Neural Networks **2**, 143 (1989).
[2] D. D. Coon and A. G. U. Perera, Appl. Phys. Lett. **51**, 1086 (1987).
[3] D. D. Coon and A. G. U. Perera, Int. J. IR Millimeter Waves **8**, 1037 (1987).
[4] H. C. Liu, Appl. Phys. Lett. **60**, 1507 (1992).
[5] D. D. Coon and A. G. U. Perera, Appl. Phys. Lett. **55**, 478 (1989).
[6] M. P. Shaw, V. V. Mitin, E. Scholl, and H. L. Grubin, *The Physics of Instabilities in Solid State Electron Devices* (Plenum, New York, 1992).
[7] D. D. Coon, S. N. Ma, and A. G. U. Perera, Phys. Rev. Lett. **58**, 1139 (1987).
[8] S. M. Sze, *Physics of Semiconductor Devices*, 2nd ed. (Wiley, New York, 1981).
[9] N. F. Mott, *Metal-Insulator Transitions* (Barnes and Noble, New York, 1974).
[10] H. C. Liu, Z. R. Wasilewski, M. Buchanan, and H. Chu, Appl. Phys. Lett. **63**, 761 (1993).
[11] Zh. I. Alferov, O. A. Mexrin, M. A. Sinitsyn, S. I. Troshkov, and B. S. Yavich, Sov. Phys. Semicond. **21**, 304 (1987).